Available online at www.sciencedirect.com
ScienceDirect
International Journal of Heat and Mass Transfer 50 (2007) 1559–1568
International Journal of HEAT and MASS TRANSFER
www.elsevier.com/locate/ijhmt

Maximum heat flux propagation velocity during quenching by water jet impingement

Aloke Kumar Mozumder, Peter Lloyd Woodfield, Md. Ashraful Islam, Masanori Monde *

Department of Mechanical Engineering, Saga University, 1 Honjo-machi, Saga 840-8502, Japan

Received 19 January 2006
Available online 7 November 2006

Abstract

Maximum heat flux propagation characteristics during quenching of hot cylindrical blocks with initial temperature 250–600 °C have been investigated experimentally using a subcooled water jet. When the wetted area starts moving towards the circumferential region, the heat flux reaches its maximum value and the position of maximum heat flux follows the visible leading edge of the wetting front. If wetting starts immediately after the jet strikes the surface, the velocity of this maximum heat flux point increases with the increase of jet velocity and subcooling and decreases with the increase of block initial temperature. These trends are opposite if there is a long delay before movement of the front.

Keywords: Quenching; Wetting front; Maximum heat flux; Impinging jet

1. Introduction

Quenching is widely used for controlling the mechanical and metallurgical properties of materials in the manufacturing industry and it is important for cooling of high power electronic chips. Also, during a loss of coolant accident (LOCA) in a nuclear power plant, quenching can be used as an effective cooling process. In spite of these important applications, understanding of the field of quenching and wetting front propagation is far from a mature science.

For jet impingement quenching of high temperature surfaces it has been found that when the liquid jet is first impinged on the hot surface it does not spread over the whole surface immediately [1–3]. Instead, it remains on a small central region for a certain period of time (depending on the experimental conditions) and splashes from this region before covering the entire surface. During the movement, the front edge of the visible moving liquid on the surface is described as the wetting front by Mozumder et al. [3] and the same definition is used in the present study. After the jet impingement and before the wetting front starts moving (i.e. during the wetting delay period [4] or resident time [1–3,5,6]), the combination of thermodynamic and hydrodynamic conditions is not suitable for complete and continuous wetting by the impinged liquid. A repeated cycle of wetting, film boiling and rewetting has been speculated to occur during this time [1,2].

Experimental and analytical investigations of jet quenching have been conducted by several other researchers [7–10] who observed many interesting phenomena during quenching. The mechanism for wetting is very important since the heat flux can be over an order of magnitude greater once wetting starts. Gunnerson et al. [4] for example, defined a criterion of rewetting as direct liquid–solid contact and the establishment of a liquid–solid–vapor triple interface. According to their investigation, rewetting required a contact angle or triple interface to be reestablished, and the liquid must recontact the solid substrate.

* Corresponding author. Tel.: +81 952 28 8608; fax: +81 952 28 8587.
E-mail addresses: 03ts11@edu.cc.saga-u.ac.jp (A.K. Mozumder), peter@me.saga-u.ac.jp (P.L. Woodfield), ashraful@me.saga-u.ac.jp (Md. Ashraful Islam), monde@me.saga-u.ac.jp (M. Monde).

0017-9310/$ - see front matter © 2006 Elsevier Ltd. All rights reserved.
doi:10.1016/j.ijheatmasstransfer.2006.08.035

Nomenclature

q_{max}	maximum heat flux (MW/m^2)	T_w	surface temperature (°C)
q_w	surface heat flux (MW/m^2)	u	jet velocity (m/s)
r	position in the radial direction of the block (mm)	u_q	maximum heat flux (MaxHF) propagation velocity (m/s)
r^*	radial position of wetting front up to resident time (mm)	z	axial distance of the block measured from the test surface (mm)
r_q	radial position of q_{max} (mm)		
t	time (counted from the impingment of jet) (s)	*Greek symbols*	
t^*	resident time (s)	ΔT_{sub}	liquid subcooling (K)
T_b	initial block temperature (°C)	λ	thermal conductivity (W/mK)

If the liquid–solid interface temperature attained upon contact equals or exceeds a thermodynamic limiting superheat of the rewetting liquid, the liquid is repelled from the hot surface and rewetting cannot occur. Many, if not most, other studies also associate the conditions required for wetting to start or the wetting front to move with an apparent 'wetting temperature'. However the range of suggested temperatures required for wetting is vast and ranges from solid superheats less than 100 °C to temperatures even beyond the critical temperature for the fluid for water [10]. Exactly what decides this temperature or the balance point conditions for deciding the wetting front velocity is still an open question.

The wetting delay period is described as resident time by Mozumder et al. [2]. This wetting delay period is also very close to the time gap between the first striking of jet and the time when the highest maximum heat flux occurs during the quench. For example in [2] after elapsing of the wetting delay period, the wetting front started moving and the surface temperature dropped immediately, which was accompanied by a dramatic increase of surface heat flux. Mozumder et al. [3] also investigated the characteristics of maximum heat flux (MaxHF) during quenching. They proposed a factor on the basis of material properties for making a relation between maximum heat flux from transient quenching experiments and critical heat flux (CHF) from steady state quenching experiments conducted by Monde et al. [11].

Barnea et al. [12] conducted a theoretical and experimental analysis of quenching propagation for a heated vertical channel with subcooled water as the working fluid. They noted that as the quench front progressed along the flow channel; it removed heat from the hot surface by several heat transfer mechanisms such as axial conduction and radial convection and radiation to the coolant. They noticed two types of flow regimes downstream of the quench front. At high inlet velocities the dominant flow regime was inverted annular flow where a liquid core flowed at the centre of the channel surrounded by a vapor annulus. At lower inlet flow rates an inverted slug flow regime typically prevailed. In both cases, the two-phase mixture downstream of the quench front acted as a precursory heat sink, which gradually decreased the surface temperature prior to quenching.

Filipovic et al. [13] conducted transient boiling experiments with a preheated copper test specimen exposed to a rectangular water wall jet on its top surface. They defined quench front velocity as the velocity at which the front sweeps along the hot surface. Their investigation revealed that increased subcooling and flow velocity accelerated propagation of the quench front. They attributed this to intensifying the rate of energy removal in the wet portion of the test specimen. They also found that higher initial test specimen temperatures resulted in smaller wetting front velocities. This can be understood in that increasing the amount of energy stored in the specimen increases the time needed to extract energy and, thus reduces the quench front velocity. Another important phenomenon disclosed from their investigation was that the quench front velocity increased as the front propagated along the test specimen. They explained this observation by noting that the specimen temperature in the precursory cooling zone ahead of the wetting region decreases with time resulting in an increased velocity of the front as it propagates along the surface.

Hammad [5] conducted experiments with the same experimental setup of the present study. The experiment was performed for the blocks with initial temperature from 250 to 300 °C and the average wetting front velocity was estimated on the basis of video images. Radial position averaged wetting front velocities for short resident time conditions were presented. The study showed that the average wetting front velocity increased with jet subcooling and jet velocity and decreased with increase of block initial temperature. It was also apparent that for short resident time conditions, wetting front velocity was the maximum for steel among three materials (copper, brass, steel) for the same experimental conditions.

With the movement of the wetting front, the position of maximum heat flux (MaxHF) also moves. Experimental studies on the movement of the MaxHF position are important for a clear understanding of quenching since the highest heat transfer rate and maximum temperature gradients occur in this region. For developing a theoretical

model of jet quenching, the MaxHF point and wetting front propagation are prerequisites. The objectives of the present study are to investigate the rate of movement of MaxHF point in the radial direction and to search for the parameters that dominate this propagation velocity. The surface thermal and hydrodynamic parameters together with the block inside temperature distribution and its effect on the MaxHF propagation velocity are also analyzed in this study.

2. Experimental procedure and data analysis

The major components of the experimental setup are shown in Fig. 1. At first a desired temperature of the impinging liquid is obtained and then a pump (6) is used for pumping it through a nozzle (11) of diameter 2 mm which is located centrally at 44 mm from the test surface. The jet velocity is estimated from differential pressure measured by a strain meter (16) which is attached at two points on the flow line before the nozzle.

The test block (1) is uniformly heated up to the desired temperature with three types of electrical heaters (15) mounted on the top and around the block. Sixteen thermocouples (0.1 mm wire diameter and 1 mm sheath diameter, type: CA) have been inserted at two different depths, 1.9 mm and 5 mm from the surface of the block which is 94 mm in diameter and 59 mm in height with cylindrical shape. Eight thermocouples are inserted along the radial direction at each depth. To protect the test surface from oxidation, it was plated with a thin gold layer of 5 μm thickness, which has a good oxidation resistance and thermal conductivity; $\lambda \approx 317$ W/mK. The roughness of the surface is 5–18 μm. Nitrogen gas is charged on the test surface during experiment from a cylinder (13) to maintain an inert atmosphere for minimizing the oxidation effect of the surface at elevated temperature. All the experiments are conducted at atmospheric pressure. A high speed video camera with a maximum resolution of 1280 × 1024 pixels and a maximum rate of 10,000 frames/s was employed for capturing the flow pattern during quenching. The thermocouples' signals are scanned by a data acquisition system sequentially at 0.05 s intervals with 8.0 ms needed to read all of the thermocouples using an analog–digital (AD) converter with 16-bit resolution. The estimated time lag of the response for the thermocouple is less than 0.1 s. The uncertainty for the placement of the thermocouples is estimated to be ±0.1 mm and the uncertainty for the measurement of temperature is ±0.1 °C. Full details of the experimental apparatus are described elsewhere [6].

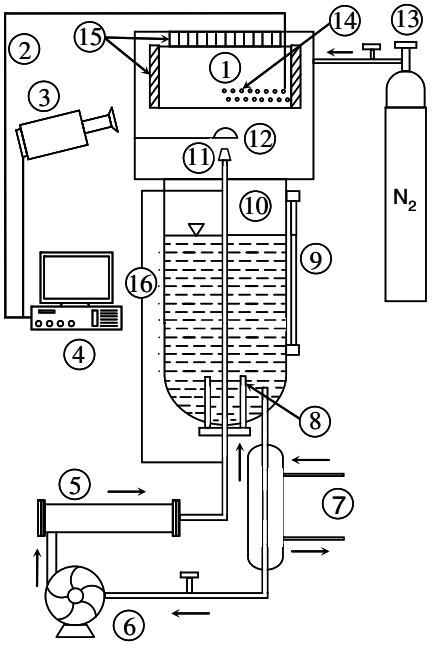

Fig. 1. Schematic diagram of the test apparatus. 1. Tested block, 2. thermocouple wire, 3. high-speed video camera, 4. data acquisition system, 5. auxiliary heater, 6. pump, 7. cooler, 8. main heater, 9. level gauge, 10. liquid tank, 11. nozzle, 12. rotary shutter, 13. nitrogen cylinder, 14. thermocouple positions, 15. block heaters, 16. dynamic strain meter (for measuring jet velocity).

Table 1
Experimental conditions

Block material	Initial temperature, T_b (°C)	Jet velocity, u (m/s)	Jet subcooling, ΔT_{sub} (K)
Steel (St), Brass (Bs), Copper (Cu)	250, 300, 350, 400, 450, 500, 550, 600 (St, Bs). 250, 300, 350, 400 (Cu)	15, 10, 5, 3	80, 50, 20, 5

Before starting of the experiment, the liquid temperature was controlled within ±1 °C and during the experiment it was sometimes noticed ±2 °C variation from the initial temperature. The jet velocity was controlled within a tolerance of ±0.1 m/s. The block initial temperature was maintained ±2 °C from the desired value. The experimental ranges for different parameters are given in Table 1.

A two-dimensional inverse solution of heat conduction was employed to estimate the surface parameters from the thermocouple readings. The inverse solution was adopted from Monde et al. [14], Hammad et al. [15] and Woodfield et al. [16]. These references describe the detailed mathematical derivation of the inverse solution and its estimation accuracy.

3. Results and discussion

3.1. Thermal parameters and hydrodynamics on the surface

As mentioned above, when the liquid was first impinged on the hot surface it remained at the small central region for a certain period of time (from fraction of a second to over 1000 s depending on the experimental conditions) before covering the entire surface. This wetting delay period is described as the resident time [2]. The radius, r^* of the small central region during the resident time is not observed to be the same for all the materials ($r^* = 5 \pm 1$ mm for copper, $r^* = 8 \pm 3$ mm for brass and $r^* \approx 1$ mm (=nozzle radius) for steel).

It is important to clarify some further terms for discussing the present quenching phenomena. Fig. 2 exhibits a video clip, surface temperature and heat flux distribution during quenching of a 400 °C steel block by 50 K subcooled liquid with 3 m/s jet. From Fig. 2 it is clear on the basis of visual observation that the liquid covers up to $r = 18$ mm in 4.8 s from the first impingement. This area of radius 18 mm is described as 'wet zone'. The outer dark area inside the wet zone is designated as 'boiling zone' which is about 4 mm ($r = 14$–18 mm) after 4.8 s for this particular experimental condition. The visible leading edge of this dark area is termed as the wetting front. This dark region is the most effective cooling zone. Due to nucleate boiling and formation of many bubbles, the video clip becomes darker in the boiling zone than in the other remaining wet zone. The temperature gradient is very high in this region and the MaxHF position also belongs to this zone (at $r = 15$ mm) as shown in Fig. 2. The temperature at the central wet region ($r = 0$–14 mm) is less than 125 °C which indicates that the possible dominating mode of heat transfer in this region is single-phase forced convection.

In Fig. 2, the region ($r = 18$–24 mm) immediate beyond the wetting front appears dry but the temperature gradient and the rate of heat transfer seem very high. The surprisingly high heat flux in this region partly may be due to limitations of the measuring technique. Due to inverse solution settings, the heat flux in Fig. 2 should be interpreted as an average over a distance of about 5 mm. This region has been marked as 'precursory cooling zone' (PCZ) as shown in Fig. 2. The term 'precursory cooling zone' is also used by Filipovic et al. [13]. Notice that in much of this region the surface temperature gradient is almost constant and pretty well corresponds to the maximum radial temperature gradient. In the present study the leading boundary of the PCZ is defined as the intersection point between a tangential line starting at the maximum radial temperature gradient position and another tangent at the position of the minimum positive radial temperature gradient ahead of the front at any instant in time (as shown in Fig. 2). In Fig. 2 this boundary occurs at about $r = 24$ mm. The definition has a convenient correspondence to the apparent 'elbow' in the radial temperature profile. It can be understood that the liquid has not yet covered this region and heat is conducted through the solid from this precursory cooling zone (PCZ) towards the inner high heat transfer boiling zone.

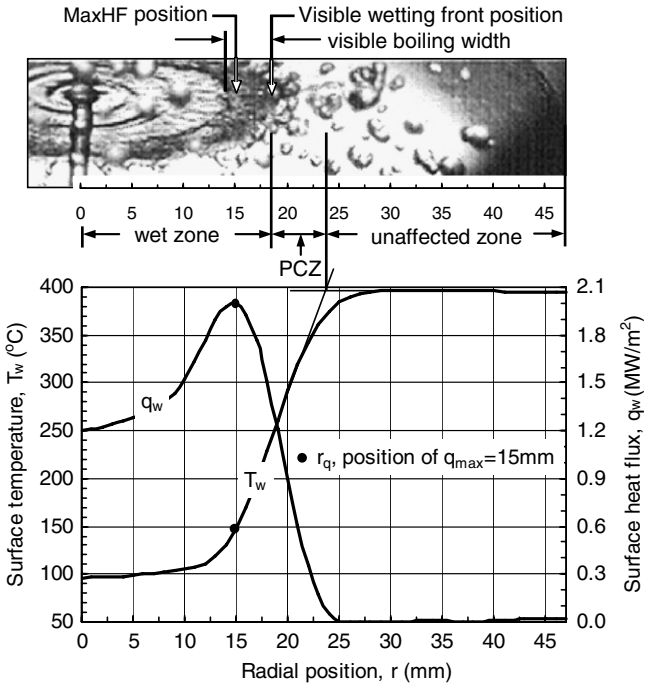

Fig. 2. Hydrodynamic phenomena on the surface together with the cooling curve and surface heat flux at $t = 4.8$ s (material: steel, $T_b = 400$ °C, $\Delta T_{sub} = 50$ K, $u = 3$ m/s).

The most outer region ($r = 24$–47 mm) is designated as the 'unaffected zone', where the surface temperature has almost the value corresponding to the time when the wetting front started moving. The heat transfer from this region is by convection to the gas phase, by radiation (which is almost negligible) and to a small extent by conduction to the supporting experimental apparatus. Most of the surface belongs to this category before the wetting front movement. It should be noted here that the example shown in Fig. 2 is for a short resident time condition. In the case of a long resident time, the surface temperature of the 'unaffected zone' actually drops down from its initial value before the wetting front movement. This temperature drop is due largely to conduction of heat towards the central region where the jet is impinging during the resident time. In this sense the whole solid is actually affected by the quench phenomena but not by the high heat flux associated with wetting. Therefore the 'unaffected zone' means here the region unaffected by wetting occurring after the resident time and exists for any resident time during the wetting front movement.

3.2. Maximum heat flux propagation

When the wetting front starts moving, the surface temperature drops sharply, a consequence of which the surface heat flux increases dramatically and heat flux reaches its maximum value. The wetting front moves from the central region towards the circumferential region and it leads the MaxHF point by a certain radial position gap as shown in Fig. 2. In Fig. 3a, both the history of the wetting front position (from the video image) and the MaxHF position are shown. Due to the limitation of the thermocouple positioning and spacing it is difficult to resolve the maximum heat flux position and hence velocity correctly for $r < 5$ mm. Therefore the results presented in Fig. 3a and b and throughout this article are for radial positions greater than 5 mm where the results are most accurate.

Fig. 3a demonstrates that the position of MaxHF always lags the wetting front by a certain radial distance, which is kept almost the same during the quench. It should be noted here that the wetting front propagation and the

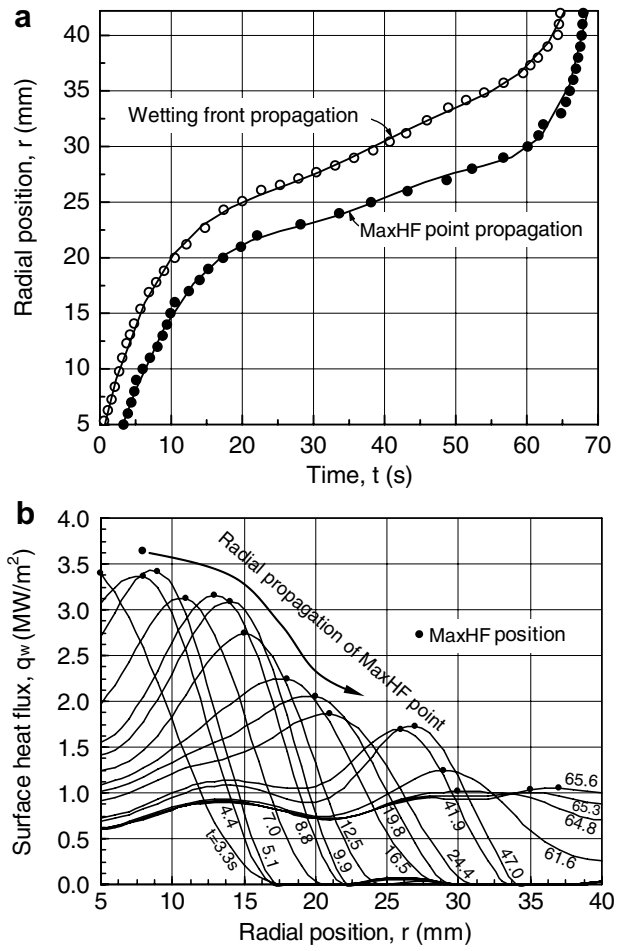

Fig. 3. Propagation of maximum heat flux (MaxHF) and wetting front position (material: steel, $T_b = 600$ °C, $\Delta T_{sub} = 50$ K, $u = 5$ m/s).

MaxHF point propagation are different phenomena but they are related and their velocity and trend in position are very close. For all cases in the present study we have found that the wetting front movement precedes the movement of maximum heat flux position. The wetting front position has been measured from the video images and the MaxHF position has been estimated from the inverse solution. The estimation of MaxHF position is easier and it is possibly more important than the wetting front position in terms of thermal stress and rapid cooling for practical applications. This is because the drastic surface temperature drop and steep thermal gradients are closely followed by and associated with the MaxHF point. For these reasons, in the present study, more emphasis will be given on the MaxHF propagation velocity (which is the rate of movement of the position of maximum heat flux with respect to time) than the wetting front velocity (which is the velocity of the visible leading edge of the moving liquid). The term 'jet velocity' represents the velocity of impinged liquid jet which is completely different from the MaxHF propagation velocity and wetting front velocity. Just at the position of the visible edge of the wetting front the probable mode of heat transfer is transition boiling while at the position of maximum heat flux the mode is nucleate boiling as reported by Mozumder et al. [3].

Fig. 3b also shows a typical heat flux distribution with radial position for different times. The solid circle symbols indicate the position of maximum heat flux at different times. It is important to note here that the MaxHF value decreases significantly with increasing radial position and time. This has been found true for a wide range of conditions [3].

To determine the MaxHF propagation velocity, the MaxHF position data are fitted by the least-squares method to a suitable polynomial and then the polynomial equation is differentiated. Fig. 4a, for example, shows the MaxHF propagation velocity as a function of radial position. The MaxHF propagation velocity for most of the cases in this study begins at a high value near the center, which decreases slowly and then more rapidly at a radial position of $r = 11 \pm 2$ mm. The MaxHF propagation velocity drops to an almost constant value around the position $r = 25 \pm 5$ mm and finally the MaxHF propagation velocity again increases sharply. The dotted circles in Fig. 4a indicate these changing trends. The pattern is typical (for most of the experimental conditions shown in Table 1) and also can be observed in Fig. 3a for both the visually observed wetting front and MaxHF point. A possible mechanism for this behavior of the MaxHF propagation velocity will be discussed below. Note here that the attained minimum MaxHF propagation velocity is often an order of magnitude smaller than the obtained MaxHF propagation velocity near the center of the test piece.

In the sections that follow we show that the bulk solid temperature when the MaxHF point starts moving has a major effect on the MaxHF propagation velocity. The jet velocity and subcooling are shown to influence both the MaxHF velocity and the resident time. Because of this double effect, increasing the jet cooling potential does not always have the expected effect of increasing the MaxHF propagation velocity.

3.3. Block initial temperature and MaxHF propagation velocity

Fig. 4a represents the variation of MaxHF propagation velocity, u_q with radial position for different block initial temperatures. The effect is dramatic. With the increase of block initial temperature MaxHF propagation velocity decreases for a given radial position. Note that for all cases in Fig. 4, the jet velocity and subcooling were the same. This result is in contrast to maximum heat flux, which is not so sensitive to the initial solid temperature for any given radial position [3]. Also the surface temperature at the maximum heat flux point for different radial positions is shown in Fig. 4b. As can be seen, the surface temperature at the MaxHF point is almost independent of the block initial temperature. With this in mind Fig. 4 leads to the almost inescapable conclusion that solid temperature is

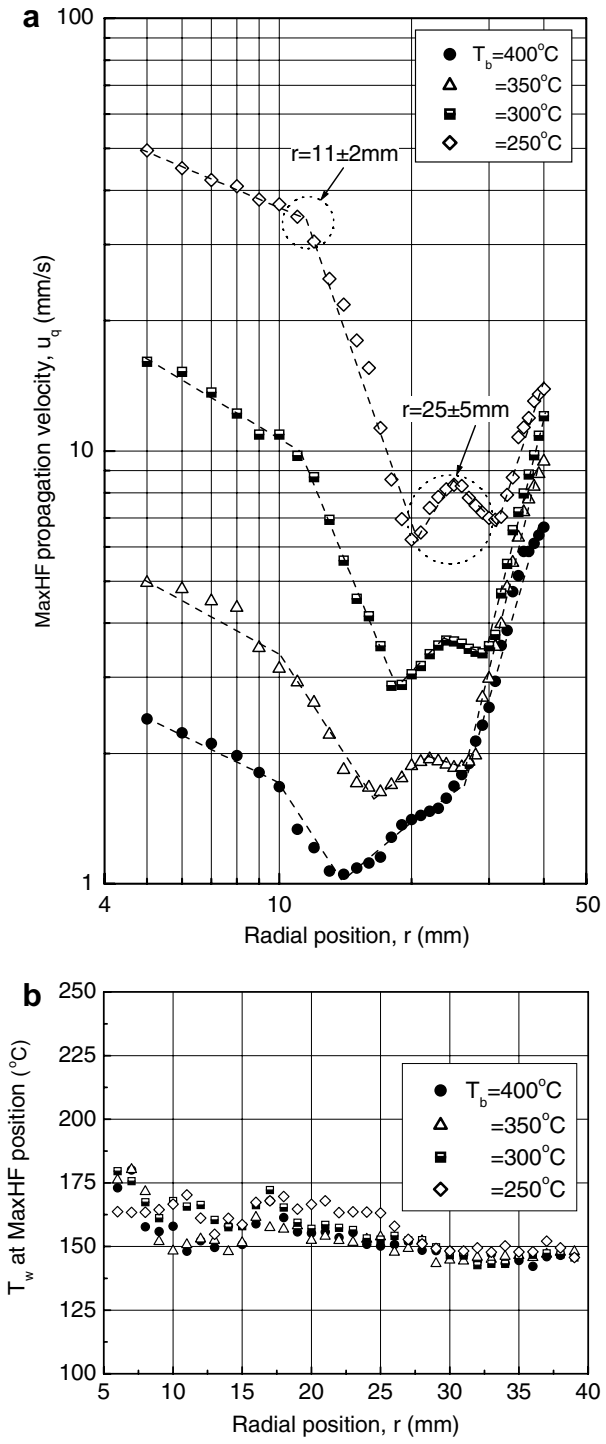

Fig. 4. Effect of block initial temperature on MaxHF propagation velocity (material: copper, $\Delta T_{sub} = 50$ K, $u = 15$ m/s, $t^* < 1$ s for all the above conditions).

important in the mechanism for wetting front propagation. The MaxHF point moves slower if the initial solid temperature is higher simply because for a similar surface heat flux it must take longer to cool the surface ahead of the wetting front. Nonetheless, it is still unclear what criteria or mechanism determines the temperature to which the surface must cool.

There is another very important factor for consideration, which is related to the initial block temperature. This is the resident time. Note that in Fig. 4a for all cases wetting started almost immediately after the jet impinged on the surface. For all the experimental conditions, the surface temperature when the wetting front starts moving is not always the same as the initial solid temperature when the jet first impinged on the surface. It entirely depends on the resident time (or wetting delay period). If the resident time is long, the surface temperature drops down during the resident time and consequently the wetting front encounters a lower solid temperature when it starts moving. Therefore, it is essential to note that the solid temperature distribution when propagation of the MaxHF point commences is more important than the actual initial temperature when the jet first impinged on the surface. Thus as will be shown below, we found that many puzzling trends in MaxHF propagation velocity could be explained well by categorizing the data on the basis of resident time.

The wetting delay period or resident time has been categorized in three groups; short resident time (less than 1 s), moderate resident time (1–200 s) and long resident time (higher than 200 s) [2]. In Fig. 5, three different regimes of resident time have been presented to get an image for the surface temperature (at $r = 5$ mm) with time. For different resident times the temperature distribution on the surface just at the time when the wetting front started moving is different. For example, the temperature at $t^* = 987$ s for the long resident time curve (a) in Fig. 5 is about 190 °C. This is over 200 °C lower than the initial temperature of 400 °C. At this time the bulk temperature for the solid is also much lower than the initial temperature. In contrast, for case (c) the wetting front starts moving in less than one second and the bulk temperature for the solid and hence most of the surface is still close to the initial temperature of 250 °C. Note that for case (c) the subcooling is greater than that for case (a) and the initial temperature is lower. Therefore without considering the resident time, we should expect that the propagation velocity would be faster for case (c) than for (a). However Fig. 5 shows the MaxHF propagation velocity is actually faster for case (a). The reason is simply that the bulk temperature of the solid is lower than 250 °C when the MaxHF point started moving in case (a) in spite of the initial temperature of 400 °C when the jet first struck the surface.

A similar story appears comparing cases (a) and (b) in Fig. 5. Both the subcooling and the velocity are higher for case (b) than for case (a). Therefore we should expect that case (b) could extract heat faster and hence have a faster propagation velocity for the MaxHF point. However, Fig. 5 reveals that for radial positions less than 30 mm, the moderate resident time case (b) has a much slower MaxHF propagation velocity than case (a). This time it is because the solid temperature is much higher for case (b) when the MaxHF point started moving than for case (a). The total time for the quench is of course much longer

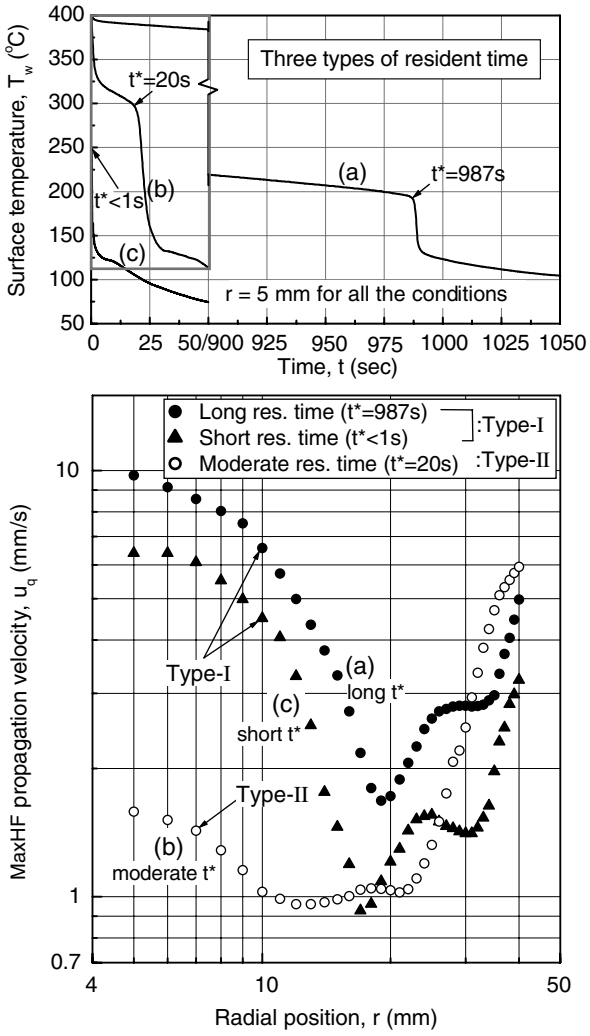

Fig. 5. Categorization of MaxHF propagation velocity on the basis of resident time. (a) Long resident time: material – copper, $T_b = 400$ °C, $\Delta T_{sub} = 5$ K, $u = 3$ m/s. (b) Moderate resident time: material – copper, $T_b = 400$ °C, $\Delta T_{sub} = 50$ K, $u = 10$ m/s. (c) Short resident time: material – copper, $T_b = 250$ °C, $\Delta T_{sub} = 80$ K, $u = 3$ m/s.

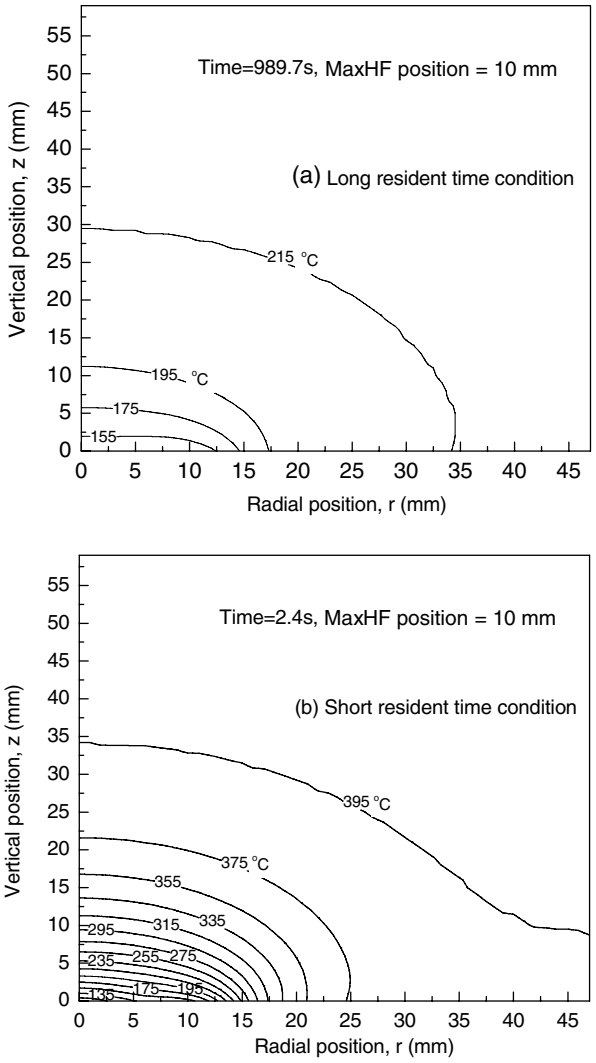

Fig. 6. Comparison of block inside temperature distribution for short and long resident time conditions. (a) Material: copper, $T_b = 400$ °C, $\Delta T_{sub} = 5$ K, $u = 3$ m/s, $t^* = 987$ s. (b) Material: copper, $T_b = 400$ °C, $\Delta T_{sub} = 80$ K, $u = 15$ m/s, $t^* < 1$ s.

for case (a) than for (b) as should be expected since the jet velocity and subcooling are higher in case (b).

Note that the shape of the MaxHF propagation velocity curve for case (b) is somewhat different to cases (a) and (c) in Fig. 5. We have labeled curves with this character as type-II while curves with the character of (a) and (c) as type-I. Generally, type-II trends in the propagation velocity occurred for moderate resident times while either short or long resident times corresponded to type-I.

It should be mentioned that it is an over simplification to talk about the solid cooling to a 'temperature' during the resident time since the temperature distribution is two-dimensional. However, it is certain that for long resident times the whole test piece does cool before propagation of the MaxHF point. Fig. 6a shows the temperature distribution in the solid about 3 s after resident time for case (a) in Fig. 5. Even though the initial temperature was 400 °C, quite clearly the whole test piece has cooled to below 250 °C. At this moment the maximum heat flux position is at $r = 10$ mm. From this point to the center, the surface temperatures are less than 155 °C. For comparison, a short resident time condition is given in Fig. 6b. Again the maximum heat flux position is at 10 mm. Clearly in Fig. 6b the bulk of the solid is still close to the initial temperature of 400 °C. From this observation we also expect that the size of the test piece will influence both the resident time and the MaxHF propagation velocity.

3.4. Effect of jet velocity on MaxHF propagation velocity

The result in Fig. 4 suggests strongly that heat transfer is a dominating mechanism for determining the propagation velocity of the MaxHF point. We should expect that any circumstances that result in stronger surface cooling will also lead to a higher MaxHF propagation velocity. However, as shown in Fig. 5, we must keep in mind that

increasing the jet velocity or liquid subcooling invariably leads to shorter resident times and hence a higher solid temperature when the wetting front starts moving. The effect of the higher solid temperature may be greater than that due to increasing the heat flux so that the unexpected effect occurs where for example increasing the jet velocity can reduce the MaxHF propagation velocity if the resident time is long.

In Fig. 7a and b, the variation of MaxHF propagation velocity with radial position for different jet velocity has been shown. Fig. 7a reveals that MaxHF propagation velocity increases with jet velocity for the short resident time conditions. For short resident time conditions (higher jet velocity and higher subcooling conditions), the wetting front starts moving immediately though most of the surface temperature is high at that time. If the jet velocity is high, the rate of heat extraction from the surface is high which results in an increase of MaxHF propagation velocity. This trend also continues up to the moderate resident time regime. On the other hand, when the resident time is long (smaller jet velocity and smaller subcooling conditions), MaxHF propagation velocity decreases with the increase of jet velocity (Fig. 7b). Within the long resident time regime, increasing the jet velocity decreases the resident time and hence the solid temperature is higher when movement of the MaxHF point commences. Therefore the MaxHF propagation velocity usually becomes slower when the jet velocity is increased in the long resident time regime.

In Fig. 7b the data for $u = 15$ m/s shows an exception to the above trend. Again this can be explained in terms of heat transfer. While the higher jet velocity resulted in a higher solid temperature in the unaffected zone when the MaxHF point started movement, the effect of the higher cooling ability of the 15 m/s jet was greater than the slowing effect of the higher solid temperature. Thus the MaxHF point moved faster for the case of $u = 15$ m/s than for $u = 10$ m/s in Fig. 7b. Exceptions such as this exist for long resident time data particularly when the resident time is reduced to close to the moderate resident time regime.

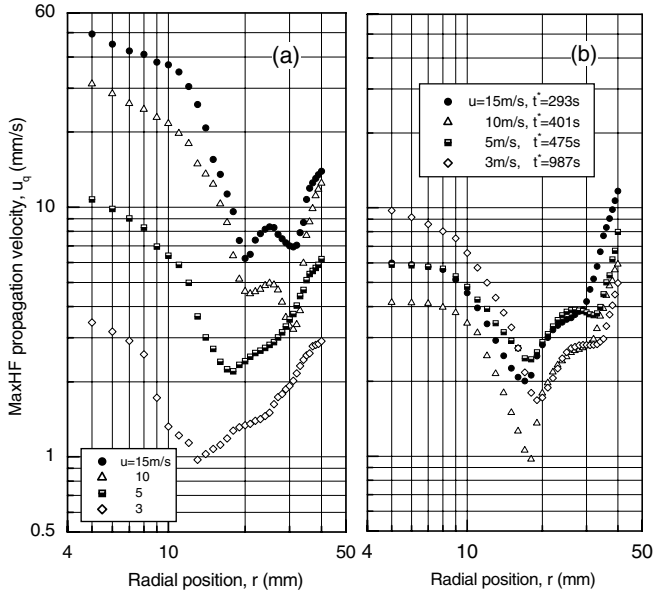

Fig. 7. Effect of jet velocity on MaxHF propagation velocity. (a) Material: copper, $T_b = 250$ °C, $\Delta T_{sub} = 50$ K (short resident time conditions). (b) Material: copper, $T_b = 400$ °C, $\Delta T_{sub} = 5$ K (long resident time conditions).

3.5. Effect of subcooling on MaxHF propagation velocity

Among various parameters, subcooling is the most dominating for the resident time [2]. Surface temperature, T_w with time for different subcoolings has been shown in Fig. 8, which also clearly represents the trend of cooling curves for different resident times. The smallest subcooling takes the longest resident time ($t^* = 987$ s) and the surface temperature at resident time is the lowest among all the

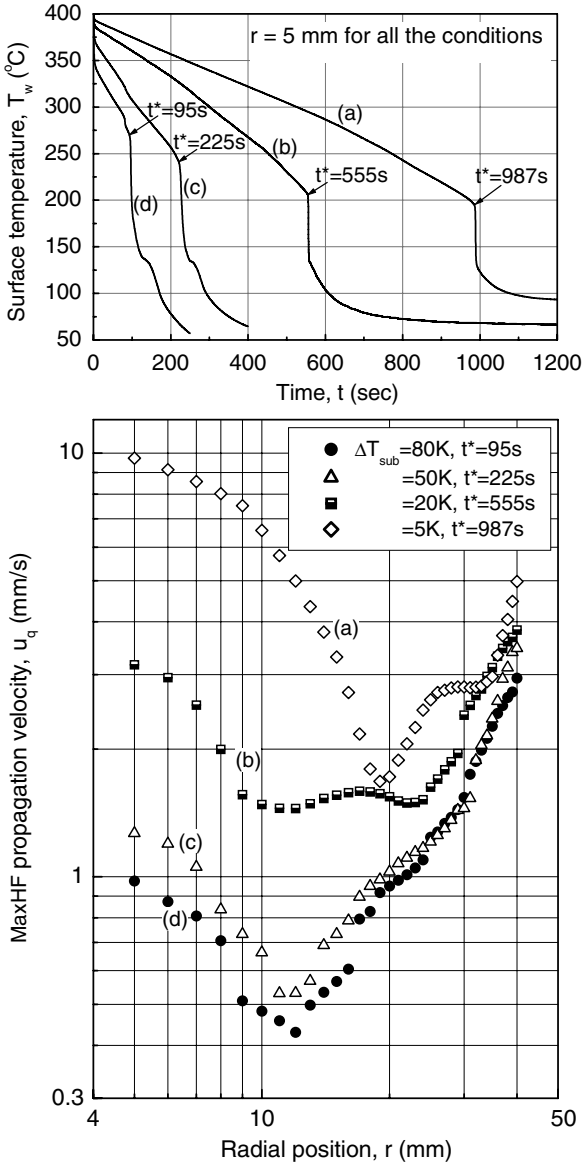

Fig. 8. Effect of subcooling on MaxHF propagation velocity (material: copper, $T_b = 400$ °C, $u = 3$ m/s). (a) $\Delta T_{sub} = 5$ K, (b) $\Delta T_{sub} = 20$ K, (c) $\Delta T_{sub} = 50$ K, (d) $\Delta T_{sub} = 80$ K.

conditions presented in Fig. 8. The variation of MaxHF propagation velocity with radial position for different subcoolings has been also represented in Fig. 8. According to Fig. 8, with the increase of jet subcooling the MaxHF propagation velocity decreases for a particular radial position. Except for (d), all the conditions in Fig. 8 belong to the long resident time regime. Smaller subcooling takes a long time for the wetting front to start movement and consequently the overall surface cooling takes place during this time, which resulted in faster propagation of MaxHF position. For this reason, higher MaxHF propagation velocity is obtained if the subcooling is lower for the long resident time regime. For the short and moderate resident time regimes, the trend is the opposite because the surface temperature in the unaffected zone when the wetting front starts moving is close to the initial temperature of the block.

3.6. Material effect on MaxHF propagation velocity

Fig. 9 represents the variation of MaxHF propagation velocity for three different materials copper, brass and steel. The data in Fig. 9 are from the same experimental conditions ($T_b = 400$ °C, $\Delta T_{sub} = 80$ K, $u = 15$ m/s) with three different materials and belong to the short resident time regime. The MaxHF propagation velocity for steel is the highest and copper has the lowest value. Due to higher conductivity of copper ($\lambda = 381$ W/mK), it can transfer heat with a higher rate but the conductivity of steel is very small ($\lambda = 37$ W/mK) which is responsible for poorer conduction of heat towards the boiling region. The conductivity of brass ($\lambda = 112$ W/mK) is in between these two materials and this order (copper–brass–steel) in relation to MaxHF propagation velocity is apparent in Fig. 9. For steel, the solid is not able to supply heat to the surface like copper or brass so a local region on the surface is easily cooled and the MaxHF point can propagate quickly. In contrast copper can supply heat quickly to the surface and the temperature and surface heat flux remain high so the MaxHF propagation velocity is lower.

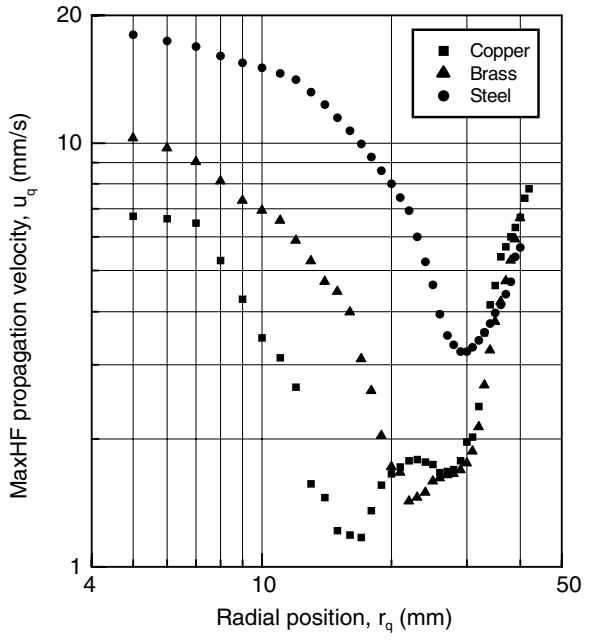

Fig. 9. Comparison of MaxHF propagation velocity for three different materials (short resident time conditions, $T_b = 400$ °C, $\Delta T_{sub} = 80$ K, $u = 15$ m/s).

In direct contrast to Fig. 9, in the case of long resident time conditions for copper, MaxHF propagation velocity is the highest for copper among all the materials for the same experimental conditions. The mechanism again relates to the temperature distribution when the MaxHF point started moving. A higher conductivity and thus a longer wetting delay for copper contribute to an overall cooling of the block prior to movement, which ultimately results in the fastest MaxHF propagation velocity among three materials.

3.7. Mechanism of MaxHF point propagation

There are many factors which may possibly influence the MaxHF propagation velocity. Some researchers place emphasis on surface wettability, hydrodynamics and the roughness or condition of the surface. However, if we assume the surface did not age much between our experiments, Fig. 4 demonstrates that with all such factors held constant, the surface temperature of the solid ranges from 175 °C to 140 °C. Therefore it is clear from this figure and the above observations that thermal effects form a dominating mechanism for propagation of the maximum heat flux point. This does not rule out the possibility of other mechanisms playing a role but it demonstrates the importance of calculating the temperature distribution within the solid and surface heat flux if one wishes to develop a suitable model.

Among those who stress the importance of temperature and heat transfer in wetting of high temperature solids, there is an argument as to which is more important, surface temperature or surface heat flux. Unfortunately the present results cannot resolve this issue because the MaxHF point is not the wetting front. Wetting starts ahead of the MaxHF point within the transition boiling region as shown in Figs. 2 and 3. It is difficult to define exactly where wetting starts and to measure the heat flux at a precise position where the surface heat flux changes rapidly. Future research may give us a more complete picture of the instantaneous heat flux and other conditions in the vicinity of the wetted region. Nevertheless we consider it is too simplistic to assume that wetting occurs at a particular surface temperature. The present results show a range of surface temperatures rather than a constant value. This is consistent with the classical boiling curve where the heat flux in nucleate boiling increases steeply within a relatively short range of temperatures.

Leaving this argument for the moment, it is worthwhile observing that heat flux and thermal considerations can

help explain the mechanism for the trend in MaxHF propagation velocity with radial position shown in Fig. 3a. Note that in Fig. 3b the heat flux decreases with radial position. Near the center of the test piece the MaxHF propagation velocity is high as a result of the high heat flux. The MaxHF propagation velocity then decreases as the heat flux decreases. While this is occurring the precursory cooling zone continuously enlarges lowering the surface temperature ahead of the MaxHF point. The reduction in surface temperature tends to cause an acceleration of the MaxHF point movement since less heat needs to be removed to cool the surface. Finally the MaxHF position accelerates even more rapidly as the PCZ reaches to the circumference of the test piece. In this region the finite solid can no longer supply heat to maintain a high surface temperature.

4. Conclusions

Due to involvement of many parameters, the maximum heat flux (MaxHF) propagation characteristics become a complicated phenomenon. More investigation is indispensable to have a clear picture for this important feature of quenching. A mathematical model and correlation have yet to be derived. The fundamental understandings at the moment are summarized as below:

1. The wetting front position is always followed by the position of MaxHF during quenching.
2. On the basis of the resident time MaxHF propagation velocity can be categorized well. For the case of long resident time, the whole block gets a cooling effect before the wetting front starts moving which favors higher MaxHF propagation velocity. The opposite is true for the short resident time.
3. MaxHF propagation velocity increases with increasing jet velocity and subcooling and decreases with increasing block initial temperature for a particular radial position in the case of short resident time. This trend is opposite when the experimental conditions are within the long resident time category.
4. MaxHF propagation velocity sequentially increases from copper, brass and steel for the same experimental conditions for short resident times. The trend is opposite for long resident time conditions (although no long resident time data for steel up to the initial block temperature 400 °C appeared in the present study), which reflects the effect of material thermal properties on MaxHF propagation velocity.
5. To develop a suitable model to correlate the data in the present article, two questions need to be addressed. Firstly; 'What triggers the MaxHF point to start moving in the radial direction?' Secondly; 'What conditions are satisfied at the MaxHF point as it moves across the surface?' The precise mechanism for the radial propagation of the maximum heat flux point has not yet been clarified. The present study did not consider the effect of the surface condition or wettability. However, a consistent pattern emerged by discussing the MaxHF propagation velocity purely in terms of thermal and heat transfer considerations.

References

[1] P.L. Woodfield, M. Monde, A.K. Mozumder, Observations of high temperature impinging-jet boiling phenomena, Int. J. Heat Mass Transfer 48 (2005) 2032–2041.
[2] A.K. Mozumder, M. Monde, P.L. Woodfield, Delay of wetting propagation during jet impingement quenching for a high temperature surface, Int. J. Heat Mass Transfer 48 (2005) 5395–5407.
[3] A.K. Mozumder, M. Monde, P.L. Woodfield, M.A. Islam, Maximum heat flux in relation to quenching of a high temperature surface with liquid jet impingement, Int. J. Heat Mass Transfer 49 (2006) 2877–2888.
[4] F.S. Gunnerson, T.R. Yackle, Quenching and rewetting of nuclear fuel rods, Nucl. Technol. 54 (1981) 113–117.
[5] J.A. Hammad, Characteristics of Heat Transfer and Wetting Front During Quenching High Temperature Surface by Jet Impingement, Ph.D. Thesis, Graduate School of Science and Engineering, Saga University, Japan, March 2004.
[6] J. Hammad, M. Monde, Y. Mitsutake, Characteristics of heat transfer and wetting front during quenching by jet impingement, Therm. Sci. Eng. 12 (1) (2004) 19–26.
[7] S.S. Dua, C.L. Tien, An experimental investigation of falling-film rewetting, Int. J. Heat Mass Transfer 21 (1978) 955–965.
[8] J.H. Lienhard, Amir Karimi, Homogeneous nucleation and the spinodal line, ASME J. Heat Transfer 103 (1981) 61–64.
[9] S. Kumagai, S. Suzuki, Y. Sano, M. Kawazoe, Transient cooling of a hot metal slab by an impingement jet with boiling heat transfer, ASME/JSME Therm. Eng. Conf. 2 (1995).
[10] J.D. Bernardin, Mudawar, The Leidenfrost point: experimental study and assessment of existing models, ASME J. Heat Transfer 121 (4) (1999) 894–903.
[11] M. Monde, K. Kitajima, T. Inoue, Y. Mitsutake, Critical heat flux in a forced convection subcooled boiling with an impinging jet, Heat Transfer 7 (1994) 515–520.
[12] Y. Barnea, E. Elias, I. Shai, Flow and heat transfer regimes during quenching of hot surfaces, Int. J. Heat Mass Transfer 37 (1994) 1441–1453.
[13] J. Filipovic, F.P. Incropera, R. Viskanta, Rewetting temperatures and velocity in a quenching experiment, Exp. Heat Transfer 8 (1995) 257–270.
[14] M. Monde, H. Arima, W. Liu, Mitutake, J.A. Hammad, An analytical solution for two-dimensional inverse heat conduction problems using laplace transform, Int. J. Heat Mass Transfer 46 (2003) 2135–2148.
[15] J. Hammad, M. Monde, Y. Mitsutake, H. Arima, Determination of surface temperature and heat flux using inverse solution for two dimensional heat conduction, Therm. Sci. Eng. 10 (2) (2002) 17–26.
[16] P.L. Woodfield, M. Monde, Y. Mitsutake, Implementation of an analytical two-dimensional inverse heat conduction technique to practical problems, Int. J. Heat Mass Transfer 49 (2006) 187–197.